

# Determination of Non-Eroding Discharge Based on the Threshold Velocity of Particle Motion and Soil Texture Triangle in Irrigation Furrows

Nazhad Khairullah, Saina<sup>a\*</sup> and Seyyed Valilou, Mir Mahmood<sup>b#</sup>

<sup>a</sup> Agricultural Engineering (Irrigation and Drainage), Tabriz University, Iran.

<sup>b</sup> Clinical Psychology, Tehran Science and Research (East Azerbaijan Branch) Tabriz, Iran.

## Authors' contributions

This work was carried out in collaboration between both authors. Both authors read and approved the final manuscript.

## Article Information

DOI: 10.9734/ARJA/2022/v15i4369

## Open Peer Review History:

This journal follows the Advanced Open Peer Review policy. Identity of the Reviewers, Editor(s) and additional Reviewers, peer review comments, different versions of the manuscript, comments of the editors, etc are available here: <https://www.sdiarticle5.com/review-history/90315>

Original Research Article

Received 25 June 2022  
Accepted 17 August 2022  
Published 29 October 2022

## ABSTRACT

One of the common methods to prevent the erosion of the furrows' bed is to enter the water flow with a discharge less than the maximum of eroding discharge. Accordingly, it is important to determine the threshold velocity of the bed particle motion. In the current study, the average diameter of particles in each soil class was determined using 12 available classes in the soil texture triangle and then in an irrigation furrow with a fixed bed and triangular cross section, the threshold velocities were calculated using the equations provided by El-Zaemey, Novak, Nalluri and Charles Heinz Bong and compared them with proposed values of Walker et al and the US Department of Soil Conservation. The results were also compared with the Shields graph by determining the Shields parameter and boundary layer Reynolds number in the slope range of 0.5% to 1% for each soil texture class. A graph was presented based on all the above mentioned methods to simplify the use of the results. In addition to specifying the difference in velocity values predicted by different methods, the graph can be also used to determine the maximum permissible velocity in furrows.

**Keywords:** Motion threshold; irrigation furrows; non-erosion discharge; soil texture triangle; triangular cross section.

# Faculty Member and University Professor;

\*Corresponding author;

## 1. INTRODUCTION

Relatively accurate estimation of the threshold velocity of the bed particles' motion is so important in the design of stabilized channels or transition structures. Because with having the threshold velocities of the motion, the conditions can be designed for preventing the erosion and sedimentation and also one can determine the non-eroding discharge with knowing these conditions in irrigation furrows, which leads to increase the efficiency of the existing system. Sedimentation in sewage and open drains systems disrupts the collection and transition of existing runoffs. To reduce sediment, Malaysian Department of Irrigation and Drainage (DID) has suggested the minimum velocity about 0.9 m/s for the stable channels to prevent sedimentation and self-cleaning conditions (Ghani et al., 2008). Walker suggested about 8 m/min for maximum water flow rate in furrows in soft silty soils and about 13 m/min in more resistant clay and sandy soils (Walker & Skogeboe, 1987).

Studies to determine the threshold conditions of motion have been conducted by two shear stress and critical velocity methods. Shields was the first person who conducted studies on shear stress [1]. Shields examined and expressed the threshold conditions of the motion for uniform textures on a flat bed. The Shields parameter or critical shear stress is calculated from the following equation:

$$\tau_{ci}^* = \frac{\tau_{ci}}{g(\rho_s - \rho)D_i} \quad (1)$$

Where  $\tau_{ci}$  is the critical shear stress for the motion threshold of a particle with  $D_i$  diameter,  $g$  = the gravity coefficient,  $\rho$  and  $\rho_s$  are liquid and particle densities, respectively. The critical boundary Reynolds number can also be calculated from the following equation:

$$Re_c^* = \frac{u_c^* k_s}{\nu} \quad (2)$$

Where  $u_c^*$  = the critical velocity for the motion threshold that is obtained by the following equation:

$$u_c^* = \left( \frac{\tau_c}{\rho} \right)^{\frac{1}{2}} \quad (3)$$

Where  $k_s$  is the length of the boundary roughness,  $\nu$  = the kinematic viscosity. Shields showed that the equation of  $k_s = d_{50}$  is true [2].

Fig. 1 shows that the Shields graph shows a steady state graph for  $Re_c^* = 489$  and  $\tau_{ci}^* = 0.06$  in the limits of the rough turbulent flow of graph. Fig. 2 shows the limits of smooth, transitional and rough beds for the Shields graph. Gessler [3] and Miller (1977) obtained similar values of 0.046 and 0.045 for  $\tau_{ci}^*$ , respectively. But because of some flaws in the Shields graph, the scientists later corrected it. Khazime Nejad and Shafaie Bejestan investigated [1], investigated the threshold conditions in a rectangular channel in a study using a physical model and 12 non-cohesive sediment samples. They could derive a graph for channels with a gentle slope. Salem [4] demonstrated in a study the effect of bed sediment thickness on determining the threshold velocity of motion in a rectangular channel with a fixed bed. They presented their equation based on the results of previous research and observation of particle motion on the bed. Alfadi (2012) investigated in a study about the cause of deviation in Shields critical shear stress and observed values of this parameter for threshold of sediment motion. They found that the existence of vertical velocity in non-uniform flows caused this declination. Finally, they were able to determine a certain value of critical shear stress for both uniform and non-uniform flow of the sediment transition. Simoes [5] showed that this method can also be commonly used to determine threshold conditions of the sediment motion using a parameter called the number of movable particles and changing the parameters of the Shields graph. Wang et al. [6] studied experimentally the presence of submerged flexible vegetation in the open channels and found with their equation, that the threshold velocity of sediment motion in the presence of the vegetation was lower than when the vegetation does not exist.

Novak and Nalluri [7,8] showed that the threshold velocity of motion in circular and rectangular channels with rough and flat and a stable invert bed follows the following equation:

$$\frac{V_c}{\sqrt{g d_{50} (S_s - 1)}} = 0.5 \left( \frac{d_{50}}{R} \right)^{-0.4} \quad (4)$$

Where  $V_c$  is the threshold velocity of motion,  $S_s$  = sediment density,  $g$  = gravity acceleration,  $d_{50}$  = average diameter of the sediment,  $R$  = the hydraulic radius of the cross sectional area of flow.

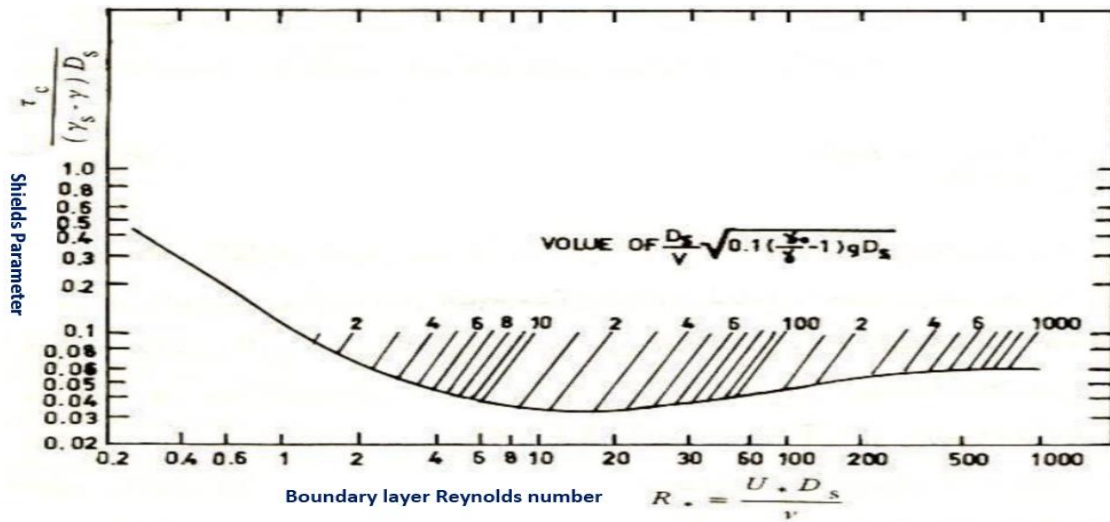


Fig. 1. Shields graph for determining Critical Shear Stress, (Vanoni, 1975)

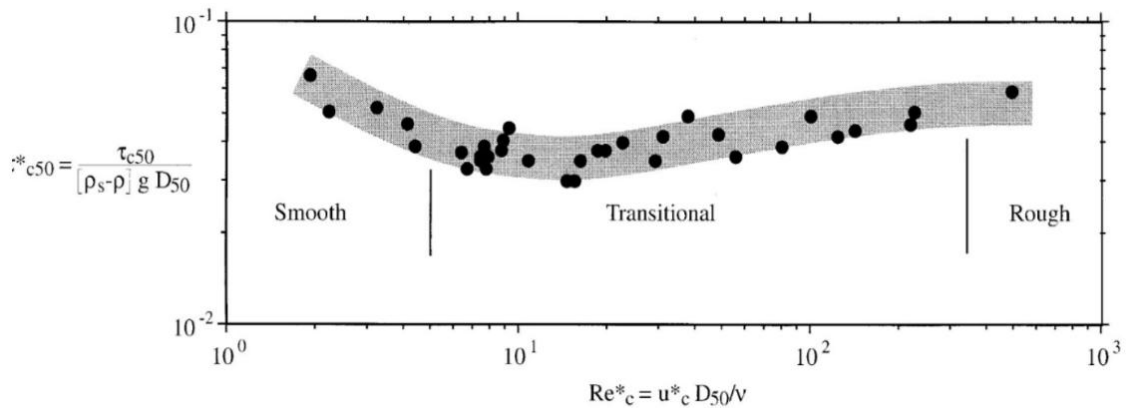


Fig. 2. Limits of available thresholds in the Shields graph (Rouse, 1939)

El-Zaemey (1991) in an experimental test on rectangular and circular channels with a flatbed showed that the critical velocity equation is the following formula:

$$\frac{V_c}{\sqrt{g d_{50}(S_s - 1)}} = 0.75 \left( \frac{d_{50}}{R} \right)^{-0.34} \quad (5)$$

Where  $V_c$  is the threshold velocity of motion,  $S_s$  = sediment density,  $g$  = gravity acceleration,  $d_{50}$  = average diameter of the sediment,  $R$  = the hydraulic radius of the cross sectional area of flow that are performed for both stable rough and flat beds.

Ghani (1999) showed that the El-Zaemey equation provides a better prediction of the critical velocity, although this equation becomes less accurate by increasing the bed thickness. Hence, Charles Hin Joo Bong

(2013) based on experimental work on a rectangular channel with three non-cohesive sediment samples at four different slopes, presented the following equation for calculating the threshold velocity of the motion:

$$\frac{V_c}{\sqrt{g d_{50}(S_s - 1)}} = 1.17 \left( \frac{d_{50}}{R} \right)^{-0.167} \left( \frac{t_s}{d_{50}} \right)^{0.0378} \quad (6)$$

Where  $V_c$  is the critical velocity,  $S_s$  = sediment density,  $g$  = gravity acceleration,  $d_{50}$  = average diameter of the sediment,  $R$  = the hydraulic radius of the cross sectional area of flow and  $t_s$  = the thickness of the sediment layer. The experiment was performed based on four thicknesses of 5, 10, 24 and  $d_{50}$ . The latter equation gives the best result for the threshold velocity of the motion.

Charles Hin Joo Bong (2013) suggested another equation based on the El-Zaemey equations (1991) and Novak and Nalluri (1984) as follows:

$$\frac{V_c}{\sqrt{g d_{50}(S_s-1)}} = 1.015 \left(\frac{d_{50}}{R}\right)^{-0.228} \quad (7)$$

Walker et al. (1987) proposed maximum water flow rates in furrows about 8 m/min in soft silty soils and about 13 m/min for more resistant clay and sandy soils.

The US Soil Conservation Service (SCS) department has proposed the following formula to determine the amount of non-eroding discharge in furrows. According to this department suggestion, the minimum slope of a furrow can be 0.5% and its maximum slope can be 1% (Alizadeh, 2014).

$$Q_{max} = \frac{0.6}{s} \quad (8)$$

Where  $Q_{max}$  is the permissible non-erosion discharge on the basis of L/S and  $s$  = the furrow slope on the basis of the percentage.

The purpose of the current study is to investigate the threshold velocity of particle motion in the irrigation furrows with different dimensions and slopes and triangular cross-section with a stabled bed with considering the variety of soil texture classes from the soil texture triangle. Therefore, it is possible to estimate the permissible velocity or maximum non-erosion discharge in irrigation furrows with a more accurate estimation according to the soil texture class compared to the conventional methods. The results have been compared with the values proposed by Walker

and Skogeboe (1987) and the formula of US Soil Conservation department.

## 2. MATERIALS AND METHODS

The furrows' cross section varies depending on the type of the selected machinery. In this study, due to the common size and shape of the soil inversion moldboard of the Furrower equipment, the triangular furrow cross section is considered. Usually furrows created by Furrower have a width between 25 and 40 cm and a height of 15 to 30 cm. In the design of the furrows, the slope is selected from 0.5 to 1%. According to the above mentioned numbers, a small cross section of the furrow (0.02 m<sup>2</sup>) and a big cross section of the furrow (0.06 m<sup>2</sup>) with 25 and 40 cm widths and 15 and 30 cm depth, respectively, were considered and two slopes within the permissible limits with considering the upper and lower limit values for each furrow. The mean values of the average diameter of the soil particles were obtained from the available 12 classes in the soil texture triangle (Fig. 3) and using the weighted average method separately for each soil texture class as follows:

Using the definition of each soil texture class in the soil texture triangle, the percentages of sand, silt and clay in each class was multiplied by the average of the diameter of each particle and finally their sum was chosen as the mean diameter of the intended soil texture class. Sediment density was considered equal to 2.6. The obtained diameter range' average of the soil and the diameter mean's average of the soil for each soil texture class are presented in Table 1.

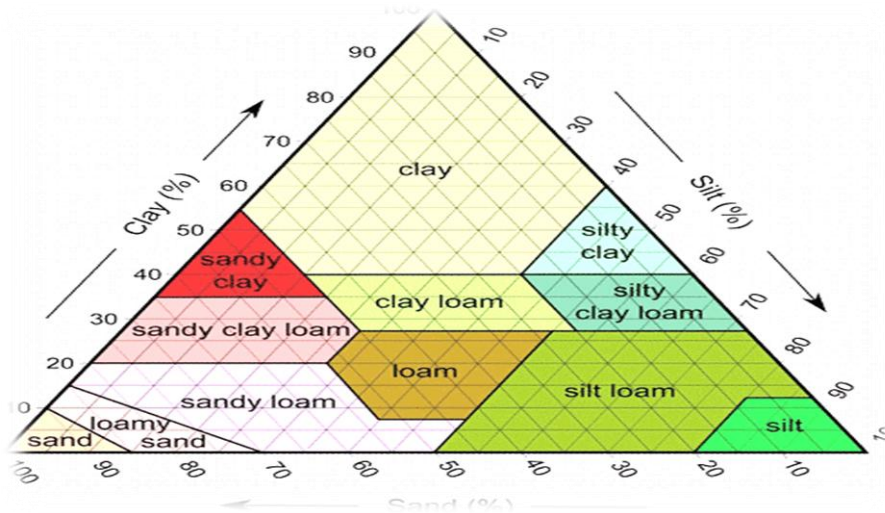


Fig. 3. Soil texture triangle

**Table 1. Particle diameter's average per soil texture class**

No:	Soil texture class	Percentage of silty clay loam	Range of $d_{50}$	$D_{50}^*$
1	Loam	85<	1.06-0.87	0.94
2	Sandy-Loamy	30> 15< 70-90	0.72-0.93	0.82
3	Sandy clay loam	20-35 28> 45<	0.47-0.91	0.69
4	Clay & Sandy	35-40 - 35-40	0.36-0.67	0.51
5	Loamy- Sandy	7> 50> 24-52	0.45-0.54	0.5
6	Loam	7-27 50-28 52>	0.25-0.54	0.4
7	Clay	40< 40-45> 40-45>	0.02-0.46	0.24
8	Silty	27-40 20>	0.01-0.2	0.11
9	Silt	12> 80> -	0.02	0.02
10	Loamy-Silty	12> 50-80 -	0.19-0.02	0.02
11	Clay & Silty	40> 40> -		
12	Loamy & Clay	27-40 20-45 -	0.01	0.01

\* $d_{50}$  is the average of particles

### 3. FINDINGS AND DISCUSSION

Shields parameter values (Equation 1) and boundary Reynolds number (Equation 2) were calculated by placing mean diameters ( $d_{50}$ ) of particles in each soil texture class and two cross-sections for irrigation furrow. Then, using the Shields graph, corresponding depths of the above values were selected as the depths of the threshold velocity of the motion. Tables 2 and 3 show corresponding depths of the threshold velocity of the motion for 0.5% and 1% slopes, respectively. As can be seen for certain values of the Reynolds number and Shields parameter as well as due to linear relationship of depth with Shields parameter, the corresponding depth of the critical velocity for the 0.5% slope has been obtained twice its corresponding values in 1% slope.

Using Equations 4 to 7 and placing corresponding depths of the threshold velocity of the motion (Tables 2 & 3), threshold velocity values of the motion were determined corresponding to each soil texture depth and class.

The texture class of soils that marked with star (\*) in the above tables was not included in the Shields graph range due to having a small mean diameter ( $d_{50}$ ). Therefore, their threshold velocity of the motion was only calculated using Equations 4 to 7 and using two considered cross-sections for furrows, and the Shields graph is not applicable for stated (\*) soil texture classes with small  $d_{50}$ .

Tables 4 and 5 and corresponding graphs (Figs. 4 and 5) show the values of the threshold velocity of the motion based on the obtained threshold depths of the motion (Tables 2 & 3) and by placing them in Novak and Nalluri

equations (4), El-Zaemey, and Charles Hin Joo Bong (6 & 7) for the soil texture triangle classes. In addition, the horizontal lines such as velocities of 0.133 m/s and 0.216 m/s of the recommended values by Walker and Skogboe (1987) are for the texture soft silt and resistant clay and sandy textures, respectively. The values of the threshold velocities of the motion calculated by all four methods at 0.5% slope are smaller than the values at 1% slope.

As can be seen in Fig. 4, the graphs of the Charles Hin Joo Bong equations are correspond to each other and have a higher bound of the threshold velocities of the motion than the other two equations (El-Zaemey, Novak & Nalluri).

As can be seen, at the threshold velocity of the motion in sandy soil texture class (0.221 m/s), the obtained values by the Charles Hin Joo Bong equations are very close (almost equal) to the suggested Walker values (0.216 m/s). At the critical velocity of resistant clay textural class, this velocity is lower (0.124 m/s) and almost corresponds to the lower bound of the suggested Walker velocity for the soft soils (0.133 m/s) and threshold velocities of the motion of the other classes of the soil texture are between these two values (0.124 to 0.221 m/s). For all available soil texture classes in Fig. 4 (except for sandy soil texture), Walker's suggested lower bound for soft soils is within the average bound of the Charles Hin Joo Bong and Novak and Nalluri equations. Whereas the Walker's proposed value for resistant soils is in the higher bound of all graphs and accordingly the Figure, the velocity of 0.216 m/s can erode the bed of all available soil texture classes (Except for the sandy soil texture class). In general, so it can be inferred that the graphs of the Charles Hin Joo Bong equations are in the average range of the two suggested values of Walker.

**Table 2. Results of boundary Reynolds number calculation, Shields parameter and corresponding depth of the threshold velocity of the motion in 1% slope**

No:	Soil texture class	Boundary Reynolds number	Shields parameter	Depth of water (cm)
1	Sandy	0.94	0.14	2.05
2	Sandy-Loamy	0.82	0.16	2.04
3	Loamy-Sandy	0.5	0.25	2
4	Loam	0.43	0.34	2.2
5	Loamy-Silty*	-	-	-
6	Silt*	-	-	-
7	Loam, Clay-Sandy	0.68	0.18	2
8	Loamy & Clay*	-	-	-
9	Loam, Clay-Silty*	-	-	-
10	Clay & Sandy	0.5	0.24	2
11	Clay & Silty*	-	-	-
12	Clay	0.24	0.54	2

**Table 3. Results of boundary Reynolds number calculation, Shields parameter and corresponding depth of the threshold velocity of the motion in 0.5% Slope**

No:	Soil texture class	Boundary Reynolds number	Shields parameter	Depth of water(cm)
1	Sandy	0.94	0.14	4.1
2	Sandy-Loamy	0.82	0.16	4.08
3	Loamy-Sandy	0.5	0.25	4
4	Loam	0.43	0.34	4.4
5	Loamy-Silty*	-	-	-
6	Silt*	-	-	-
7	Loam, Clay-Sandy	0.68	0.18	4
8	Loamy & Clay*	-	-	-
9	Loam, Clay-Silty*	-	-	-
10	Clay & Sandy	0.5	0.24	4
11	Clay & Silty*	-	-	-
12	Clay	0.24	0.54	4

**Table 4. Calculated threshold velocities of the motion ( $m0s^{-1}$ ) in furrows and at 0.5% slope**

	Sand	Sandy Loamy	Sandy clay Loam	Clay, Sandy	Loamy-Sandy	Loam	Clay
El-Zaemey,	0.04	0.036	0.031	0.024	0.024	0.019	0.013
Novak	0.158	0.155	0.152	0.147	0.147	0.15	0.138
Charles 1	0.212	0.202	0.19	0.172	0.171	0.161	0.134
Charles 2	0.212	0.204	0.194	0.179	0.178	0.171	0.147

**Table 5. Calculated threshold velocities of the motion ( $m0s^{-1}$ ) in furrows and at 0.1% slope**

	Sand	Sandy Loamy	Sandy clay Loam	Clay, Sandy	Loamy-Sandy	Loam	Clay
El-Zaemey,	0.04	0.036	0.031	0.024	0.024	0.019	0.013
Novak	0.158	0.155	0.152	0.147	0.147	0.15	0.138
Charles 1	0.212	0.202	0.19	0.172	0.171	0.161	0.134
Charles 2	0.212	0.204	0.194	0.179	0.178	0.171	0.147

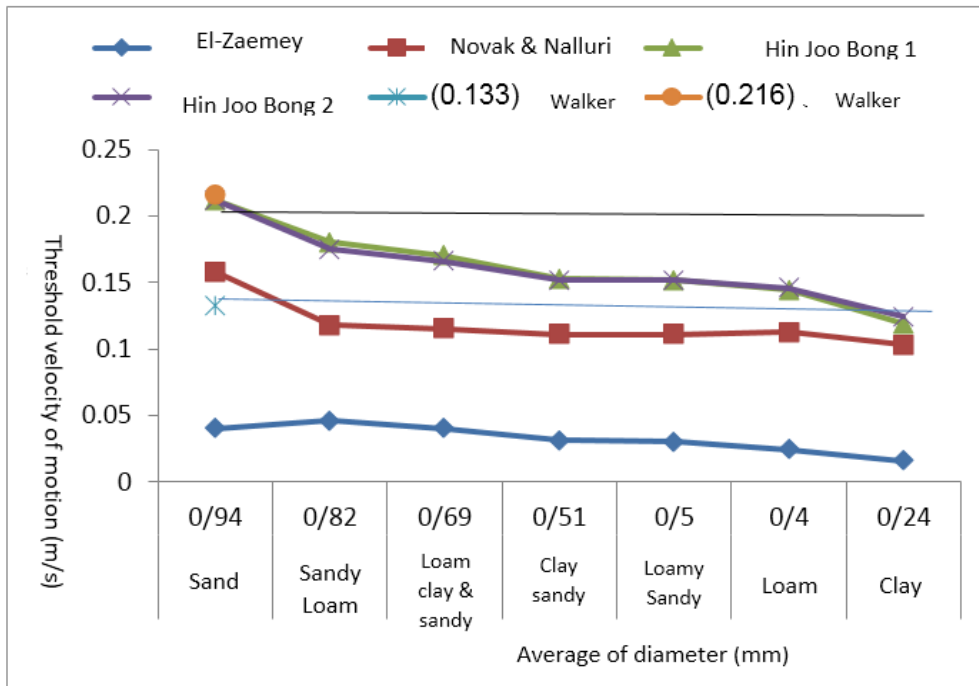


Fig. 4. Comparison of values of calculated threshold velocities of the motion with proposed values for furrow with 0.5% slope

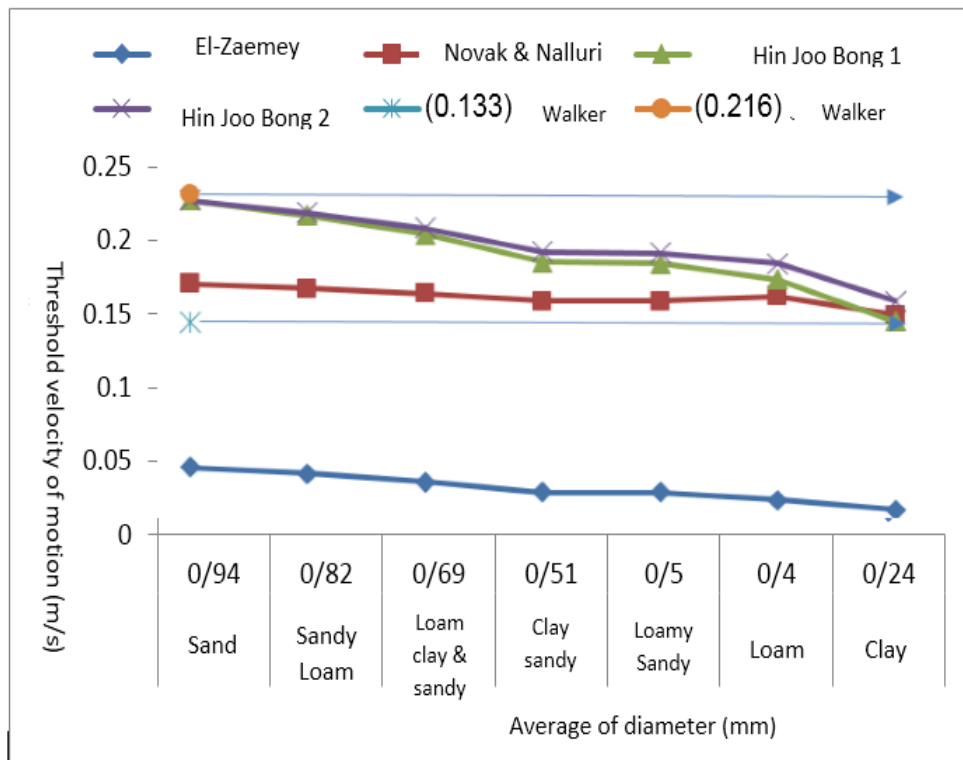


Fig. 5. Comparison of values of calculated threshold velocities of the motion with proposed values for furrow with 0.1% slope



As can be seen in Fig. 5, the equations of Charles Hin Joo Bong correspond to one another, and finally, these graphs (clayey texture class) correspond to the graphs of Novak & Nalluri equation. All three of these equations are within the range of Walker's proposed figures. All three of these equations show that the bed of all existing soil textural classes began to move at velocities greater than 0.133 m/s and less than 0.216 m/s.

In both Figures, all equations are in descending order, and by decreasing the average diameter of the soil texture class, the threshold velocity of motion decreases as well.

Due to the small average diameter in some soil texture classes, it is not possible to determine the threshold depth through the Shields graph, therefore, it is determined by hypothetical areas of the furrow (0.02 and 0.06 m<sup>2</sup>) (Figs. 6 & 7).

Comparison of the calculated threshold velocities of motion for furrow with the Walker proposed velocities (0.133 m/s) in erodible soils and in the non-erodible soil (0.216 m/s) shows the obtained figures from the four used Charles Hin Joo Bong equations are close to the Walker values for the loamy-silty, silt, loam clay and clay silty classes

in the tables of the values for the obtained threshold velocities of the motion. Walker presented the two digits with a high confidence coefficient, therefore it can be the reason for the existing small discrepancy between the proposed of Walker values for the threshold velocity of the motion and the obtained values.

Fine and coarse particles of the soil co-exist in the nature with each other, and placing fine-grained particles among coarse-grained particles leads to increase resistance of the soil against the erosion. In the present study, the average diameter of particles in each soil texture class was calculated based on the soil texture triangle so that the diameter and the percentage of the fine and coarse particles in each soil class were taken into account, which can increase the threshold velocity of the motion and reduce soil erosion. As we know, by increasing the threshold velocity of water motion and the possibility of entering a flow with larger discharge in the irrigation furrows, the distribution uniformity increases and it leads to the efficiency of the irrigation system, but it requires a precise determination of the threshold velocity of the motion by considering the soil-grading and the irrigation furrows conditions (slope, threshold area, etc.).

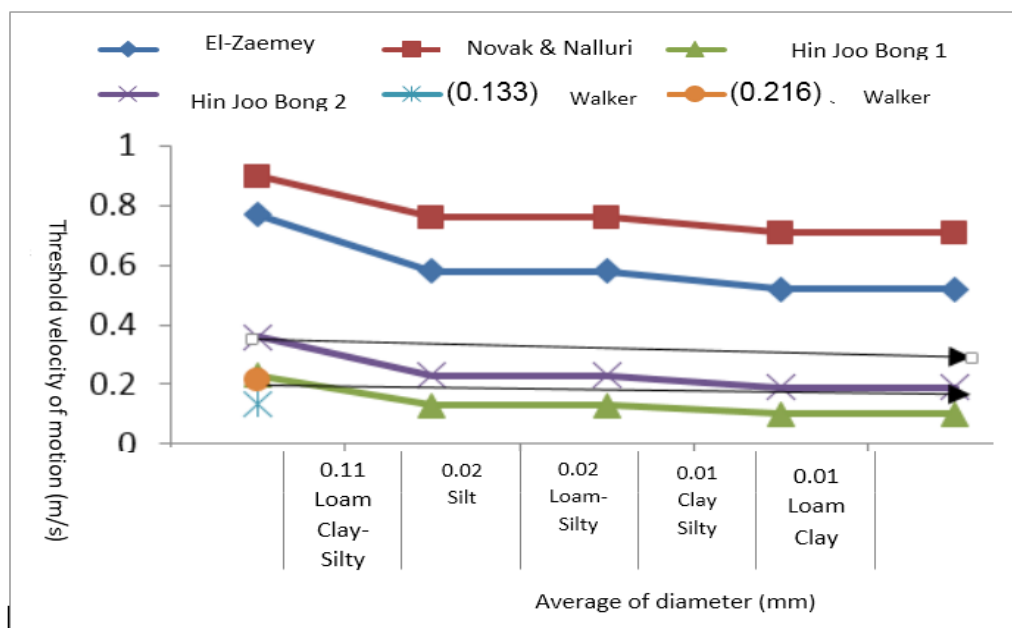


Fig. 6. Comparison of values of calculated threshold velocities of the motion with proposed values for furrow with an area of 0.02 (m<sup>2</sup>)



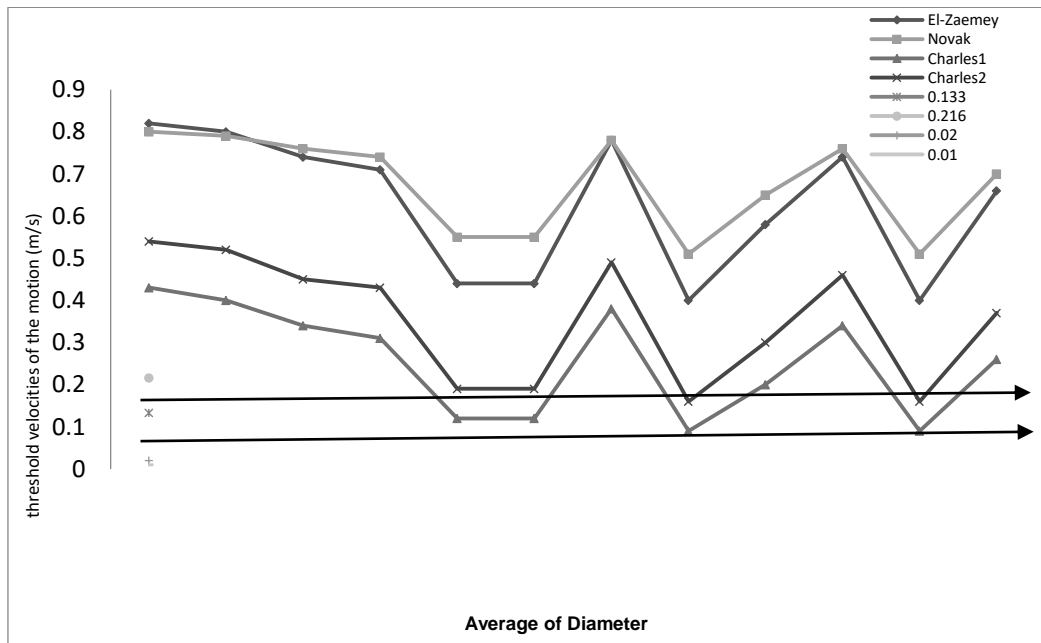


Fig. 7. Comparison of values of calculated threshold velocities of the motion with proposed values for furrow with an area of 0.06 (m2)

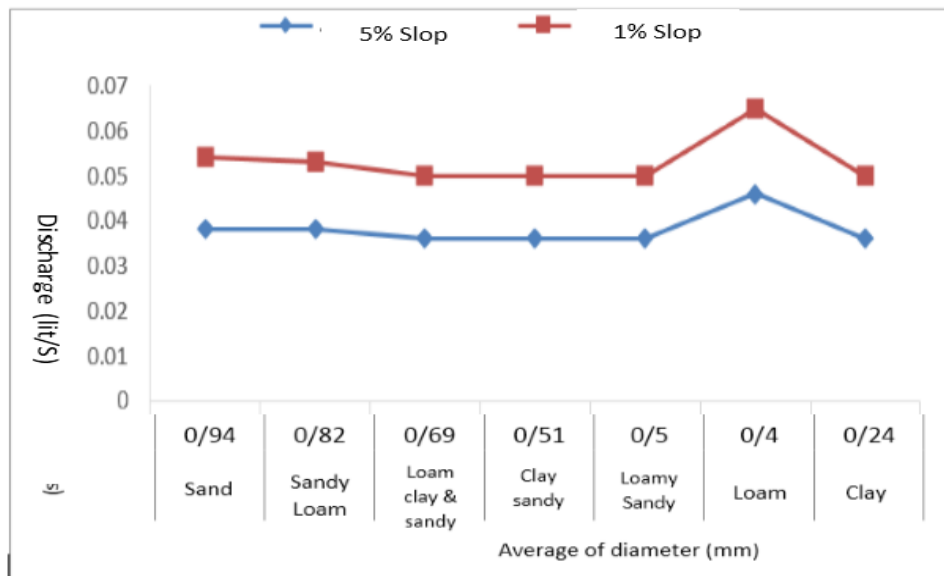


Fig. 8. Calculated Non-eroding discharge values based on threshold velocities of the motion

Table 6. Discharge values in furrows using the scs equation

Discharge (lit s <sup>-1</sup> )	Slope (%)
0.5	1.2
1	0.6

### 3.1 Manning Formula and Determination of Non-eroding Discharge

With having the threshold velocities of the motion for each soil texture class and assuming that the

entering flow rate is constant with a certain texture in a furrow, the non-eroding discharge can be determined using the Manning equation.

Also, the maximum non-eroding discharge proposed by SCS is 1.2 and 0.6 lit/s for the furrow with a small slope (0.5%) and a large slope (1%), respectively, with respect to the considered limit slope for the furrows.

#### 4. CONCLUSION

By looking at the graphs, one can be seen that Walker's suggested values are in the lower and middle range of these graphs and these numbers are stated very conservative. Almost all soils are eroded at values above the critical velocity of 0.133 m/s. The obtained graphs from the Charles equations are more cautious than the L-Zaemey and Novak and Nalluri equations. Therefore, the obtained values of the current study are recommendable in the practical works for better and more accurate design of the graphs use.

#### COMPETING INTERESTS

Authors have declared that no competing interests exist.

#### REFERENCES

1. Khazime Nejad H, Shafaie Bejestan M. Investigation of threshold conditions of non- Noncohesive sediments' motion in open channels with gentle slope and rectangular cross-section. Scientific Journal of Irrigation and Water Engineering, First year. 2010;2:13-23.
2. Montgomery DR, Buffington JM. Channel-reach morphology in mountain drainage basins. Geological Society of America Bulletin. 1997;109(5):596-611.
3. Gessler J. Beginning and ceasing of sediment motion. River Mechanics. 1971; 1(1):7-1.
4. Salem AM. The effects of the sediment bed thickness on the incipient motion of particles in a rigid rectangular channel. InProc. 17th Int. Water Technology Conf., IWTC17, Istanbul, Turkey; 2013.
5. Simões FJ. Shear velocity criterion for incipient motion of sediment. Water Science and Engineering. 2014;7(2):183-93.
6. Wang H, Tang HW, Zhao HQ, Zhao XY, Lü SQ. Incipient motion of sediment in presence of submerged flexible vegetation. Water Science and Engineering. 2015;8(1):63-7.
7. Novak P, Nalluri C. Incipient motion of sediment particles over fixed beds. Journal of Hydraulic Research. 1984;22(3):181-97.
8. Alizadeh A. Principles of Designing Irrigation Systems in the farm, Chapter 9. 1393;351.

© 2022 Saina and Mahmood; This is an Open Access article distributed under the terms of the Creative Commons Attribution License (<http://creativecommons.org/licenses/by/4.0>), which permits unrestricted use, distribution, and reproduction in any medium, provided the original work is properly cited.

*Peer-review history:*

*The peer review history for this paper can be accessed here:*  
<https://www.sdiarticle5.com/review-history/90315>